ELSEVIER

Cement & Concrete Composites 23 (2001) 247–254

Cement & Concrete Composites

www.elsevier.com/locate/cemconcomp

Distances between air-voids in concrete by automatic methods

Anne-Sophie Dequiedt *, Michel Coster, Liliane Chermant, Jean-Louis Chermant

LERMAT, URA CNRS 1317, ISMRA, 6 bd Maréchal Juin, 14050, Caen Cedex, France

Abstract

In order to access to the air-void distances in concrete by automatic image analysis, three different methods were proposed, used and discussed: half-distances between two voids nearest neighbours, called count-dilation; half-distances between all neighbours, called SKIZ; and distance function. They were utilized in a euclidean and geodesic way. Some of them can replace favourably the manual methods proposed in the different standards.

Keywords: Air-void distance; Dilation-counting method; Skeleton by influence zone method; Distance function method; Automatic image analysis

1. Introduction

The presence of air-void in concrete has a great influence on the frost resistance [1]. It depends on the air-void content, their size and their dispersion in concrete [2]. Their dispersion is generally characterized by the half-distance between voids, in the literature parameter $\bar{L}$, [3–5] which is directly linked to the frost resistance [6]. Two standards [7,8] can be used to determine this half-distance. They are based on the model of Powers [9] where any measure of distance is necessary (see Appendix A), but all these measurements are undertaken by manual methods.

To avoid errors linked to manual methods some automatic ones are proposed in this work to determine these distances between voids. They represent the distance for the water to reach a void. So if one considers that water cannot move through gravel, the distance between air-voids can be defined according to euclidean and geodesic concepts [10]. The geodesic concept in mathematical morphology will be presented in Appendix B, for those who are not familiar with.

In a previous work one has shown that the presence of gravel does not affect the dispersion of air-voids in the cement paste, in a relevant way [11]. The scope of this work is to show if sand has an influence on these distances. This investigation has been performed at a microscopic scale.

2. Tested materials

The materials used for this study are some test blocks of micro-concrete (Table 1). Gravel used has a size distribution between 3.5 and 6.3 mm, while that of the sand is limited to 4 mm. In fact one considers these coarse and/or aggregate particles as gravel. After one month of curing, specimens were cut in thick slices. These slices were embedded in an epoxy resin (Struers, Copenhagen, Denmark) under vacuum, and ground up to 3 μm.

3. Image acquisition

Image acquisition was made from a scanning electron microscope (SEM), (JEOL JSM 6400, Tokyo, Japan). Two types of images were used: (i) backscattered electron images (BEI) (Fig. 1), where the air-voids (resin) appear in black and then can be easily segmented; (ii) but that is not the case for the gravel and sand; so a second type of image has to be used; as gravel and sand are rich in silica, their segmentation will be made from the silicon map-making (Fig. 2).

Magnification used is × 50. This choice is due to a compromise as there is a great dynamics of size in this class of materials. In these conditions, the choice of the magnification was checked as allowing for the longest inter air-void distances to be fully included within the frame of measurements. In these conditions for a 512×368 pixels^2 image, the pixel size equals 5 μm, and then image size is 2.56×1.84 mm^2. Fifty frames of

* Corresponding author.

0958-9465/01/$ - see front matter
PII: S0958-9465(00)00055-X

Table 1
Composition of the investigated specimens

Cement ($g\ l^{-1}$)	Gravel ($g\ l^{-1}$)	Sand ($g\ l^{-1}$)	w/c (wt)	Air entraining additive % of cement weight
450	800	1200	0.5	0.03

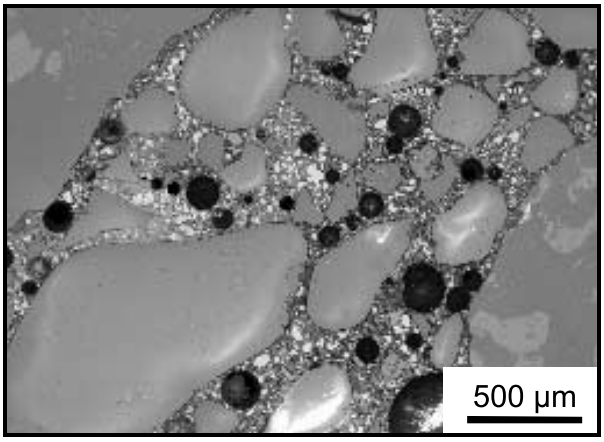

Fig. 1. Backscattered electron image of a classical concrete.

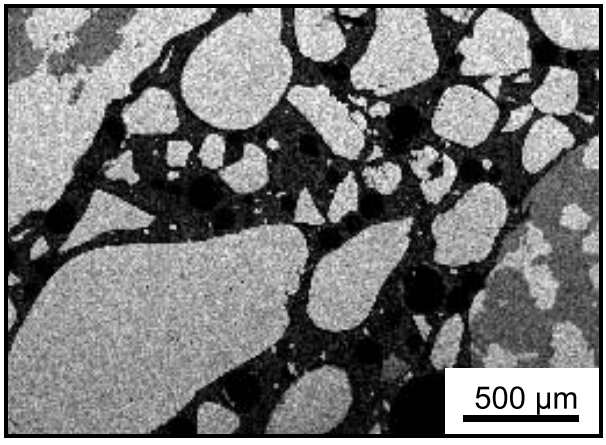

Fig. 2. Image of the same area as in Fig. 1, but from the silicon map-making.

measurements were analysed in the direction perpendicular to the casting axis and 50 frames in the direction parallel. But as these results were equivalent, all the following measurements have been made only on the perpendicular direction.

One must note that it is important to obtain an image with a sufficient quality for a map-making to be automatically segmented. For that purpose, one has to work at 20 kV and especially one must scan slowly and several times the samples. 25 scans were used, which correspond to half an hour to acquire one image.

4. Image segmentation

To analyze the morphology of materials by automatic methods of image analysis requires to modify the initial image to eliminate the noise and evidence the phases or features to be extracted.

Grey tone images acquired from a scanning electron microscope (SEM) generally are somehow noisy. So one has used a linear filter obtained in replacing the value of each pixel by the weighted mean of that pixel and of its near neighbours in a 3×3 window.

Then the extraction step consists of transforming the grey level image in a binary one. The determination of the optimum grey level threshold is performed automatically. Several methods can be used.

For our images, the better one is the method proposed by Kölher [12]. It is based on the contrast analysis of the image. For each potential threshold, s, the mean contrast associated, $\bar{C}(s)$, is calculated according to the following relationship:

$$\bar{C}(s) = \frac{\sum_{k(s)} \min\left(|g(x) - s|; |g(y) - s|\right)}{\text{card } K(s)},$$

with $g(x)$ and $g(y)$ the values of x and y neighbour pixels, surrounding the threshold s, $K(s)$, the pair of associated pixels, as Ks corresponds to the number of pairs in $K(s)$. The retained pixel is that which will give a maximum value for $C(s)$.

Unfortunately all the defects are not eliminated by this grey tone threshold. The objects of very small size are considered as noise and will be eliminated by an opening-reconstruction of size 2, [13,14], (this concept is explained in this issue [15]). A hole filling will allow to suppress the image background noise. Finally an opening of size 1 will smooth the outline of the objects.

If some air-voids are connected, a segmentation with a watershed method will be used [16,17], (this concept is also explained in this issue [15]). Fig. 3 illustrates the obtained result in Fig. 1.

5. Analysis of distance between air-voids

Two processes were developed to investigate the distance between air-voids. Another investigation was performed at the macroscopic scale [11]. In this paper, several methods would be proposed to determine the distribution of distances at the microscopic scale. Two methods give the distribution of distances between two voids nearest neighbours (individual analysis and count-dilation methods) and lead to similar results. So as count-dilation method is fasted, individual analysis method will not be presented here. Another method will concern the analyses of distances between all

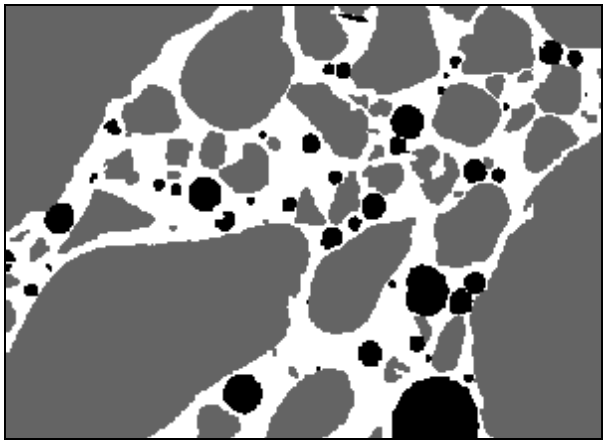

Fig. 3. Image of a concrete, with the three binary phases separated: air-voids in black, gravel and sand in grey, and matrix in white.

neighbours, and the last one the map-making of distances between one point of concrete to a void. These three methods will be resumed.

Two ways can be used to study the distances between air-voids: the first one is by a euclidean or classical manner on all the image, and for the second one, the geodesic way, where one considers that water cannot move through gravel and sand, so in these conditions one uses geodesic distances in the complementary set of gravel and sand (see Appendix B).

The geometrical definition of the different parameters p, r, d, measured from these three methods is shown in Fig. 4.

5.1. Method 1: distribution of half-distances between two voids nearest neighbours (Count-dilation method)

A method derived from the Shehata's method [18] was chosen. Its principle consists of calculating the number of particles which stay isolated after a certain number of dilations. The size of dilation corresponds to the half-distance which separates two voids, which corresponds to $p/2$.

In concrete terms, void set is dilated. From the obtained image, one substracts the initial image. Then one obtains holed particles. If the number of holes is greater than 1, the particle corresponds to connected voids. So multiple points of the complete thinning by the structuring element D [13,19] are used to serve as markers to reconstruct connected voids. By difference, one obtains isolated voids. Indeed, only voids connected by dilation give thinned images with multiple points (Fig. 5).

Thus, to each dilation the number of non-connected particles is recorded. Its variation allows to obtain the distribution of individual particles which disappear as a function of the dilation size. A geodesic version of this algorithm has been developed: the euclidean dilation is then replaced by the geodesic dilation of voids in the matrix.

This method was called "count-dilation".

5.2. Method 2: distribution of half-distances between all neighbours (SKIZ method)

The half-distance between voids can also be achieved in studying the skeleton by influence zone (SKIZ) of voids (Fig. 6). This concept is explained in this issue [15]. Thus, after elimination of the SKIZ multiple points, the voids are dilated step by step by a euclidean or geodesic way until the reconstruction of segments of this SKIZ. For the geodesic version, the geodesic SKIZ of voids in the complementary set of gravel and sand is used. When a segment is reached, it is reconstructed and substracted to the binary segment image. The disappearance frequency of segments according to the dilation size is thus obtained. In any case, the theorem of the mask of

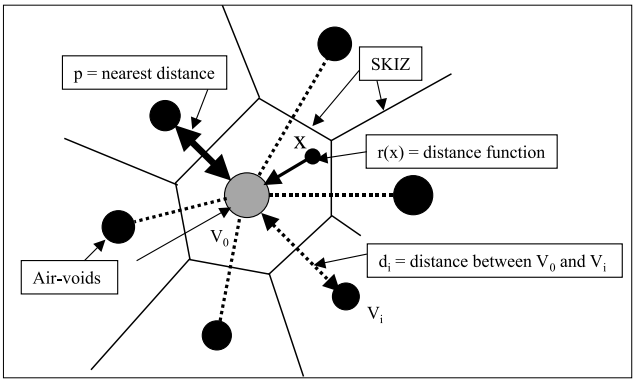

Fig. 4. Meaning of the three different parameters measured. Air-voids are represented by circles in black and in grey for the pore taken into consideration for the measurements.

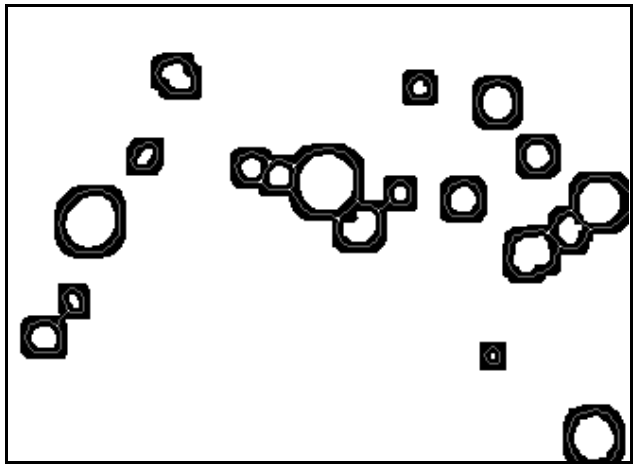

Fig. 5. Illustration of the count-dilation method.

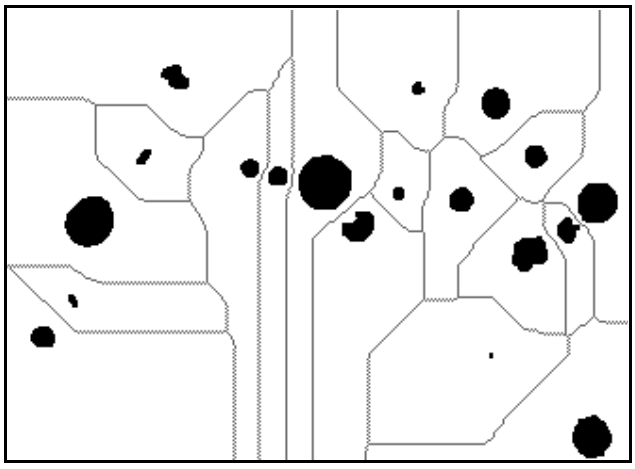

Fig. 6. Illustration of the skeleton by influence zone (SKIZ) method.

Fig. 7. Image of the adaptative mask to investigate the geodesic distance function.

measurements was used to reduce the border effect [19] as the size of the frame is reduced according to the size of the distance to be analysed.

With methods 1 and 2, the air-void distances are always calculated inside the cement paste, and not in the gravel (as there is no way for the water!).

5.3. Method 3: distribution from the distance function

The last method utilized is the distance function in the complementary set of voids [20]. It allows to characterize the distribution of distances from a point of the concrete to a void.

For the distance function, r, as for the count-dilation, p, and SKIZ, d, methods, but in a way much more sensitive, one can make the measurements taking into consideration either the full frame of measurements (gravel+cement paste+air-voids) or only the cement paste+air-voids. For the previous defined parameters, Dequiedt has shown [21] that the use of euclidean or geodesic methods give similar results as the nearest air-voids are always visible between them in the cement paste. On the contrary for the distance function all the points of the images are taken into consideration. As the number of points which belong to gravel is important, it introduces a bias (as there cannot be water in gravel): then the euclidean distance function must be excluded. So one presents here only the geodesic distance function method. This method leads to a problem regarding the edge of the frame of measurements. To solve this, one has used a geodesic mask of measurements in which the measurements of geodesic distances are not biased. So the next steps will be:

- calculation of the geodesic distance function of the mask of measurements in itself,
- calculation of the geodesic distance function of voids in the complementary set of gravel and sand (image F),

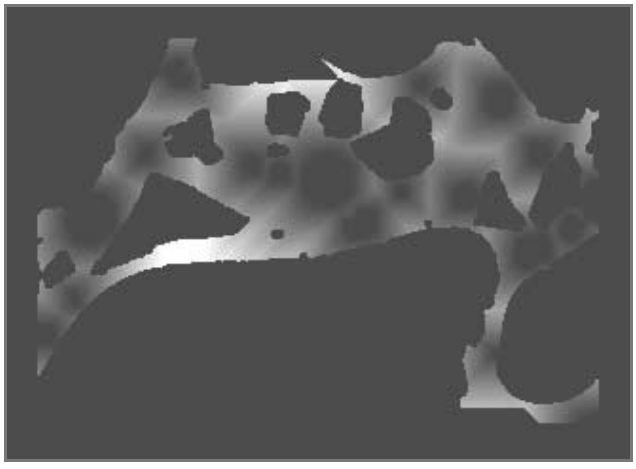

Fig. 8. Image of the geodesic distance function of the air-voids in the adaptative mask.

- substraction of these two images,
- threshold between 1 and 255 (image M), (Fig. 7),
- multiplication of the image F by the image M, (Fig. 8).

The histogram of the distance function gives the geodesic distance distribution. Then same parameters as before can be calculated.

6. Results

For each analysis method used, a graph of the distance distribution and its histogram are given (Fig. 9). They were obtained after the analysis of a minimum of 50 images. Some significant parameters are resumed in Table 2.

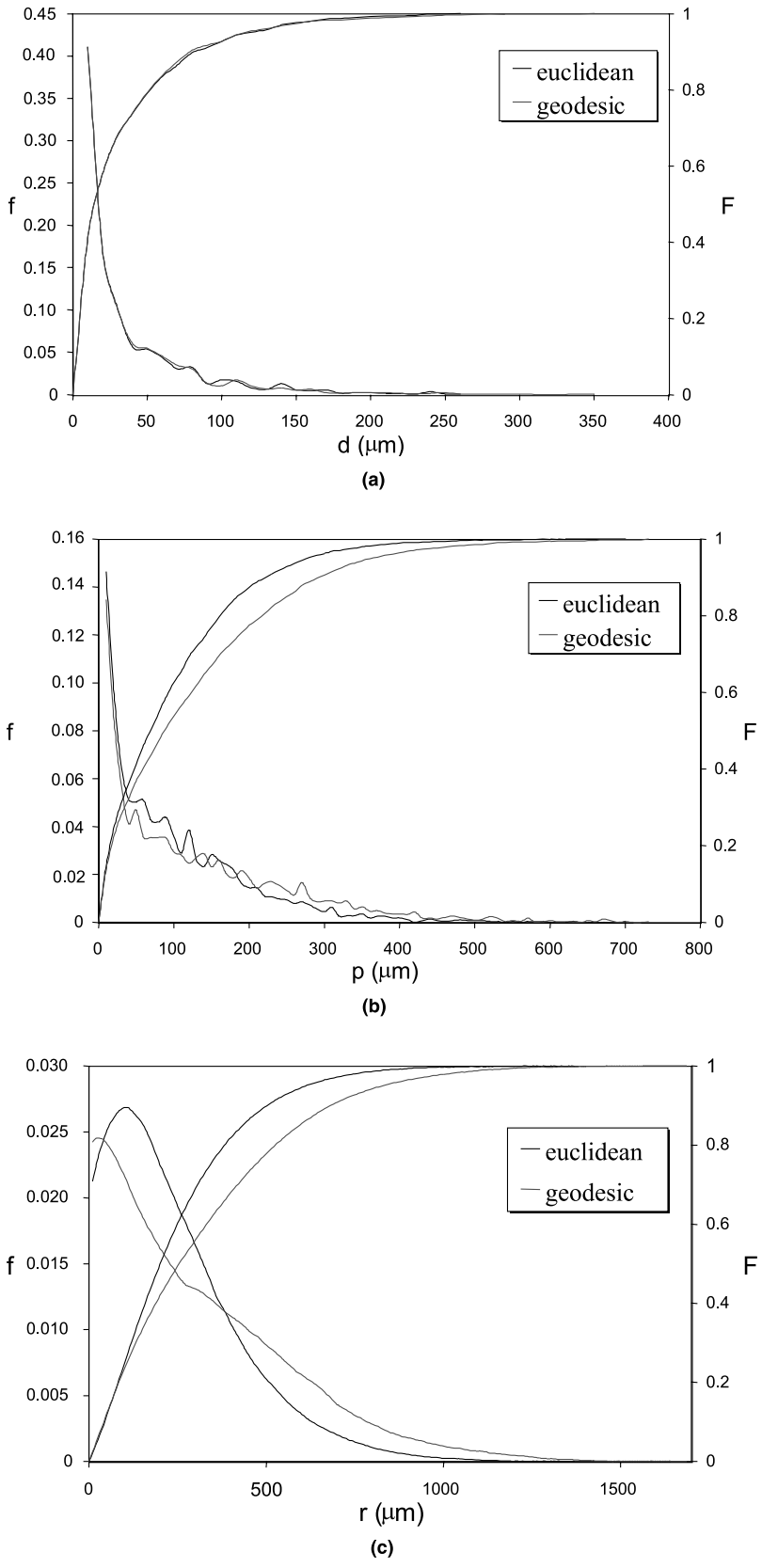

Fig. 9. Distributions of distances between air-voids d, p, r according to the three proposed methods, respectively count-dilation, SKIZ, and distance function (f: granulometry density; F: cumulated distribution): (a) Count-dilation method; (b) SKIZ method; (c) Distance function.

Table 2
Characteristical parameters of the distance distributions

$\bar{d}$ (μm)	Half-distance between two voids nearest neighbours ($p/2$)		Half-distance between neighbours (SKIZ) ($d/2$)		Geodesic distance from one point of the matrix to a void (r)
	Euclidean	Geodesic	Euclidean	Geodesic	
	33.5	33.5	97.6	127.2	161.4
$\sigma/\bar{d}$	1.20	1.24	0.95	0.98	0.81
$\sigma_1/\bar{d}$			0.49	0.49	0.46
$\sigma_2/\bar{d}$	0.82	0.82	0.74	0.79	0.67
$\sigma_3/\bar{d}$			2.20	2.26	1.98
$\sigma_4/\bar{d}$			1.23	1.28	1.12

7. Discussion

In this discussion we shall first present a comparison of the different proposed methods, and then compare the results with the proposals of the classical standards.

7.1. Comparison of the different methods

One notes first that the distributions of distances between two nearest neighbours voids by euclidean and geodesic ways are identical. If one looks carefully for these distributions, one notes that the results are approximately the same for euclidean and geodesic measurements for the first 1/3 of the distribution, which corresponds to a size up to 15 μm. This means that the magnification is too low to see small distances. So quartile cannot be calculated. This problem leads to an error on the mean value. However if one wants to analyze geodesic distances in the complementary set of gravel and sand, a greater magnification cannot be used. Otherwise the covariance of gravel does not reach its asymptotic value.

For the distance function, the fact that gravel and sand are not taken into consideration for the euclidean results leads to an opposite result. These elements present a great surface area, so, using the euclidean function, all these points are considered like matrix points, but they are not represented using the geodesic function. In consequence the euclidean mean value is higher than that given by the geodesic method. If one considers that in concrete water cannot move inside gravel, this euclidean method must be excluded

For the study of the distances between all neighbours, the mean value is higher than from the previous method. But the geodesic mean distance is greater than the euclidean one. However the distributions stay similar: their reduced quartiles and standard deviation are identical.

One has shown that the distance between two nearest air-voids is biased, due to a problem linked to the choice of magnification. To solve this problem one has chosen to represent the distance distribution between nearest neighbours by a theoretical law.An exponential law seems to be convenient (Fig. 10). Its mean value gives an order of magnitude for the mean distance value between

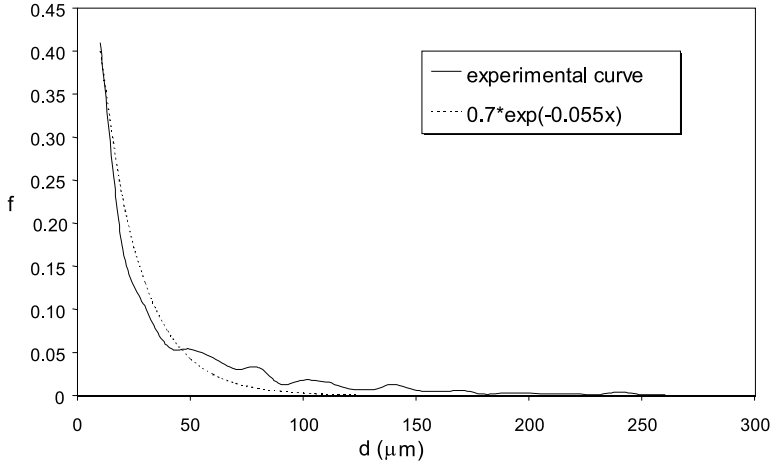

Fig. 10. Modelling of the count-dilation curve by an exponential law.

two nearest neighbours, close to 12.5 μm. It corresponds to 1/3 of the mean value obtained experimentally. The choice of the exponential distribution permits to obtain a value certainly rather closer to the reality than the mean value calculated from the previous distribution. However this result must be confirmed.

7.2. Comparison with ASTM C 457-90 standard

To validate this study one has compared our results on half-distances between voids with those obtained from the ASTM C 457-90 standard. However this standard advocates a manual method to determine air-void and cement paste contents, and number of voids. In this work, one has chosen to calculate these parameters by an automatic method. One uses a linear analysis like in the standard, but on the SEM images and not on images obtained with an optical microscope.

The length across air-voids and cement paste, $\bar{L}$, and the number of voids are calculated. They allow to determine the air-void and cement paste contents and the specific surface area of air-voids. One obtained a value for $\bar{L} = 131.6$ μm.

This value must be compared with those obtained with our automatic methods (Table 2). $\bar{L}$ seems to correspond to the geodesic half-distance between all neighbours. It appears that the results for the geodesic distance function (SKIZ) gives quite close result as those from the standard. This is interesting because this method is very rapid. The SKIZ methods are, geometrically, the closest measurement of the standard as with the standard one has a regular tessellation of the space, while with the SKIZ method the tessellation is random.

8. Conclusion

The study of the air-void distance distributions in concrete is important regarding the freeze-thaw frost resistance of these materials. One has then proposed three automatic methods to characterize this dispersion, using euclidean and geodesic processes: a method based on count-dilation, on the skeleton by influence zone, and on the distance function.

The different results show that the distribution of the nearest neighbours is the same by euclidean or geodesic method. This means that the nearest neighbours are not influenced by gravel and sand in the cement paste.

Moreover the skeleton by influence zone method which takes into account all the nearest neighbours shows the sand influence as the geodesic distance is always higher than that measured by a euclidean way. Conversely to gravel, sand grains isolate the air-voids.

Moreover one of our methods, the geodesic SKIZ one, gives results closest to those obtained from ASTM C 457-90 standard, as geometrically it is the closest. So it appears to be the best method used to automatically measure the mean length across air-voids and cement paste according to the ASTM C 457-90 standard.

Acknowledgements

This work was performed in the frame of the "Pôle Traitement et Analyse d'Images", Pôle TAI, (Pôle of Image Processing and Analysis) of Basse-Normandie, France. One of the authors (ASD) was supported by the Ministère de l'Education Nationale, de la Recherche et de la Technologie.

Specimens were elaborated at ESITC, Groupe ESTP, Epron: we want to thank this School of engineers for allowing us to use their facilities.

Appendix A. Power's model

To determine the half-distance between air-voids in concrete (parameter $\bar{L}$), Powers has proposed a simple model [4,9]. In this model, the random dispersion of air-voids in the cement paste is replaced with a geometrically regular pattern of single size voids distributed in a uniform three-dimensional grid. The dimension of this cube is determined so that the volume of the air-voids with regard to the volume of "grid space" between them is equivalent to the measured volume of air with regard to the measured volume of the hardened cement paste [2]. So $\bar{L}$ corresponds to the greatest half-distance between two adjacent voids, i.e. to the distance between the center of the cube to the periphery of the nearest void. The value of this parameter is given by the Powers formula:

$$\overline{L} = \frac{3}{S'_{\mathrm{V}}(V)}\left(1.4\left(\frac{V_{\mathrm{V}}(P)}{V_{\mathrm{V}}(V)}+1\right)^{1/3}-1\right),$$

where $S'_{\mathrm{V}}(V)$ is the specific surface area of voids, as defined in civil engineering, $V_{\mathrm{V}}(P)$, the volume fraction of hardened cement paste without voids, and $V_{\mathrm{V}}(V)$, is the volume fraction of voids.

It is important to note that the definition of the specific surface area used by the civil engineers is different from that used in image analysis. In the Powers formula, the specific surface area, $S'_{\mathrm{V}}(V)$, is defined by:

$$S'_{\mathrm{V}}(V) = \frac{\text{total area of voids}}{\text{total volume of voids}}.$$

Appendix B. Geodesic methods in mathematical morphology

B.1. Euclidean morphology

Let us recall first some basements on the two basic operators in mathematical morphology: the erosion and

the dilation [13]. If the structuring element is a disk B of size λ, B_λ, the erosion will consist of keeping the points of the set which correspond to a disk totally included in the object. So a thickness of size λ will be removed from the set. The dilation is the reciprocal (dual) operation. In that case, with the same disk, a thickness of size λ is added.

The opening corresponds to an erosion followed by a dilation. The elementary erosion and dilation also allow to calculate the distance function.

B.2. Euclidean and geodesic distances

The notion of distance commonly used is the euclidean distance, classically defined as the shortest distance between two points or two sets.

For the geodesic distance a supplementary constraint is important : the way to go from one point to another must obligatorily go through a space or a set of reference. For example, the geodesic distance to go by sea between New York and San Francisco is by the Horn cape. When there exists no possible way between two points, one says that their geodesic distance is infinite.

The previous morphological operators can also be defined in a geodesic way. For example, the reconstruction is an infinite geodesic dilation.

References

[1] Atilh. Le béton exposé aux agressions hivernales. Documentation Technique No. 1, January 1989.
[2] Hover KC. Air content and unit weight of hardened concrete. In: Klieger P, Lamond JF, editors. Significance of tests and properties of concrete making materials, vol. 169C. ASTM STP; 1994. p. 296–14.
[3] Mielenz RC, Wolkodoff VE, Backstrom JE, Flack HL. Origin, evolution, and effect of air-void system in concrete. Part 1-Entrained air in unhardened concrete. Proc Amer Concr Inst 1958;55:95–121.
[4] Powers TC. Void spacing as a basis for producing air-entrained concrete. J Amer Concr Inst 1954;50:741–60.
[5] Pigeon M, Lachance M. Critical air-void spacing factors for concretes submitted to slow freeze-thaw cycles. Amer Concr Inst J 1981;78(4):282–91.
[6] Pigeon M, Plante P, Saucier F. Production et stabilité du réseau de bulles d'air entraînées dans le béton. Report from the Université de Laval, Département de Génie Civil, April 1987.
[7] Afnor nf en 480-11. Adjuvants pour bétons, mortiers et coulis – Méthode d'essais – Partie 11: Détermination des caractéristiques des vides d'air dans le béton durci. Norme Européenne, Norme Française, French standard, March 1999.
[8] ASTM C 457-90. Standart test method for microscopical determination of parameters of the air-void system in hardened concrete. December 1990.
[9] Powers TC. The air requirement of frost resistant concrete. Proc Highway Res Board 1949;29:184–211.
[10] Lantuejoul C, Maisonneuve F. Geodesic methods in image analysis. Patt Recogn 1984;17:177–87.
[11] Dequiedt AS, Redon C, Chermant JL, Chermant L, Coster M. Characterisation of diffusion paths of water in concrete by color images analysis. Acta Stereol 1999;18:227–37.
[12] Köhler R. A segmentation system based on thresholding. Comput Graphics Image Process 1981;15:319–38.
[13] Serra J. Image analysis and mathematical morphology. New York: Academic Press; 1982.
[14] Serra J. Image analysis and mathematical morphology – Vol. 2: Theoretical advances. New York: Academic Press; 1988.
[15] Coster M, Chermant JL. Image analysis and mathematical morphology for civil engineering materials. Cem Concr Comp 2001;23:133–51.
[16] Beucher S. Segmentation d'images et morphologie mathématique. Thèse de Docteur-Ingénieur, Ecole Nationale Supérieure des Mines de Paris, Fontainebleau, 1990.
[17] Vincent L, Soille P. Watersheds in digital spaces: an efficient algorithm based on immersion simulations. IEEE Trans Patt Anal Mach Intelligence 1991;13(6):583–98.
[18] Shehata MT. Application of image analysis in characterising dispersion of particles. In: Petrucks W, editor. vol. 16. Mineralogical Association of Canada: Ottawa, Canada; 1989. p. 119–32 [chapter 14].
[19] Coster M, Chermant JL. Précis d'analyse d'images. 2nd ed. Paris: Les Editions du CNRS, 1985; Paris: Les Presses du CNRS, 1989.
[20] Rosenfeld A, Pfaltz JL. Distance functions on digital pictures. Pattern Recognition 1968;1:33–61.
[21] Dequiedt AS. Contribution à l'étude morphologique des ciments et bétons par analyse d'images multimodales. Thèse de Doctorat of the University of Caen. 1999.